Supporting Information

van Baarlen *et al.* 10.1073/pnas.0809919106

SI Methods

Bacterial Culturing Conditions. To obtain stationary phase cells, 500-mL cultures of *Lactobacillus plantarum* WCFS1 (cultured at 37 °C in MRS, Merck) were used to inoculate 16 L of fresh and prewarmed MRS medium and grown overnight. Cells were harvested by centrifugation (6,000×*g*, 20 min), washed, and re-suspended in 600 mL of MilliQ. This suspension was divided in 2 equal portions; one was heat-treated (10 min at 85 °C) to obtain the "dead" bacterial preparation. To live and dead stationary phase cells maltodextrin and glucose were added to a final concentration of 20% and 2% (wt/vol), respectively. Bacterial suspensions were divided in 2–3-mL aliquots, frozen at −40 °C and then freeze-dried. To obtain mid-logarithmic growth phase cells, 250-mL cultures of *Lactobacillus plantarum* WCFS1 (overnight in MRS medium, at 37 °C) were used to inoculate 16 L of fresh and prewarmed MRS medium and cultured (37 °C) until an optical density at 600 nm of 1.0 was reached. Mid-log cells were then treated similar as stationary cells. Placebo controls were prepared by dissolving maltodextrin 20% and glucose 2% (wt/vol), in 300 mL of MilliQ and freeze-dried. Freeze-dried bacteria were stored at 4 °C. Bacterial viable counts, colony forming units on MRS-agar plates, determined for each of the bacterial preparations at the beginning and end of the intervention trial (after 4 interventions were completed in all subjects), showed that bacteria were virtually unaffected by the storage period (data not shown). The freeze-dried mid-log and stationary-phase bacterial preparations contained ≈0.8 and 0.9 × 10^{11} cfus per ml, whereas no cfus could be detected in the heat-treated variant of the same bacterial suspension, nor in the placebo preparations. Freshly prepared suspensions or placebo drinks were administered 1 × 150 mL at the start of the intervention, followed by 12 × 100 mL every 30 min, over a period of 6 h.

RNA Isolation. Total RNA was extracted from biopsies with TRIzol reagent, purified and DNase treated using the SV Total RNA Isolation System (Promega). RNA integrity was checked on an Agilent 2100 Bioanalyzer (Agilent Technologies) with 6000 Nano Chips according to the manufacturer's instructions. RNA was judged as suitable for array hybridization only if samples showed intact bands corresponding to the 18S and 28S ribosomal RNA subunits, displayed no chromosomal peaks or RNA degradation products, and had an RIN (RNA integrity number) >8.0.

Array Hybridisation and Quality Control. Total RNA (500 ng) extracted from biopsies was labeled using the Ambion MessageAmp II biotin enhanced single-round amplification kit (cat. no. 1791), hybridized to human Genome U133 Plus 2.0 arrays (Affymetrix), washed, stained and scanned on an Affymetrix GeneChip 3000 7G scanner. Detailed methods for the labeling and array hybridizations are described in the eukaryotic section of the GeneChip Expression Analysis Technical Manual, Revision 3, from Affymetrix and are also available upon request.

Array Hybridisation and Quality Control. Bioconductor (1) packages (www.bioconductor.org) integrated in the automated on-line MADMAX pipeline (https://madmax.bioinformatics.nl) were used for analyzing the scanned Affymetrix arrays. Strict quality criteria were used to obtain high-quality array data. Arrays were considered of sufficient quality when they showed not >10% of specks in Bioconductor's fitPLM model images, were not deviating in RNA degradation and density plots, were not significantly deviating in NUSE and RLE plots and were within each other's range in boxplots. For a more extensive description of quality criteria, please contact the authors.

Redefined probesets (2) were based on the Entrez Gene database, build 36, version 2; remapped CDF v9. Expression estimates were obtained after quantile normalization by robust multiarray analysis (RMA; 3). Bioconductor packages (4) (www.bioconductor.org) integrated in the automated on-line MADMAX pipeline (https://madmax.bioinformatics.nl) were used for all analyses.

Differentially expressed probesets were identified using moderated t-statistics that implement empirical Bayes regularisation of standard errors (5). *P* values were corrected for multiple testing using a false discovery rate method (6). Because the current algorithms to determine the FDR are usually too restrictive for studies in which subtle changes in gene expression are observed, application of FDR filtering will result in loss of important results (7). A cut-off of *P* value <0.05 was therefore used in this study.

Reconstructing the Biological Context of Expression Datasets. Three complementary methods were applied to relate changes in gene expression to functional changes. One method, provided via the ErmineJ software program, is based on overrepresentation of Gene Ontology (GO) terms (8). Another approach, gene set enrichment analysis (GSEA), takes into account the broader context in which gene products function, namely in physically interacting networks, such as biochemical, metabolic or signal transduction routes (9). Both applied methods have the advantage that they are unbiased, because no gene selection step is used. Moreover, since a score is computed based on all genes in a particular GO term or gene set, the signal-to-noise ratio is boosted allowing the detection of transcriptional programs that are distributed across an entire set of interacting genes yet are subtle at the level of individual genes. In addition, biological biological interaction networks among regulated genes activated in response to bacterial interventions were identified using Ingenuity Pathways Analysis (IPA) (Ingenuity Systems). IPA utilizes a large expert-curated repository of molecular interactions, regulatory events, gene-to-phenotype associations, and chemical knowledge, mainly obtained from peer-reviewed scientific publications, that provides the building blocks for network construction. IPA annotations follow the GO annotation principle, but are based on a proprietary knowledge base of >1,000,000 protein–protein interactions. The IPA output includes metabolic and signaling pathways with statistical assessment of the significance of their representation being based on Fisher's Exact Test. This test calculates the probability that genes participate in a given pathway relative to their occurrence in all other pathway annotations. Detailed descriptions of the applied methods are available upon request. Input gene lists included those genes of which the expression had changed with P values <0.05 and a fold-change cut-off of 1.1. Earlier studies (10, 11) have shown that mild stimuli induce small (10–40%) changes in gene expression in human tissue and may be a characteristic of mean expression changes in human tissues, typically consisting of multiple cell types.

Histological Evaluation of Tissue Sections. For histological examinations of Mayer's haematoxylin/0.25% eosin stained sections, light and fluorescence microscopy were performed using a Leica Laborlux S microscope equipped with Leitz Fluor and NPL Fluotar objectives, phase contrast and epifluorescence setup

(excitation/emission I2/3, excitation bandpass BP450–490, emission longpass LP515). For 3 volunteers, at least 12 sections per treatment were studied at magnifications up to 1,000× for infiltration of immune cells or tissue damage. Images were captured using a Coolsnap digital CCD camera (Photometrics). Representative images were optimized using Adobe Photoshop CS software by using the "Unsharp mask" filter option and by adjusting the yellow intensity of FITC images, using the "Curves" option. For histological evaluations and interpretations, 10–20 microscopic views (depending on cell variation in the tissue sections) at magnifications ranging from 200× to 1,000× were compared. We assumed that an inflammatory immune response could be identified easiest by searching for infiltration of immune cells, especially in regions where follicles were present. To this goal, microscopy views were screened with special attention for clusters (>3–5) of immune cells separately or cooccurring within a view. We found that microscopy views contained only few immune cells; apart from the commonly occurring B cells, only neutrophils and macrophages were observed, per view always <5–10 (depending on the magnification). To further search for signatures of an inflammatory response, sections were screened for presence of small follicles because these might more readily reveal release of higher numbers of immune cells and infiltration in neighboring tissue parts. Also such sections did not reveal higher numbers of immune cells, not in biopsies obtained after bacterial nor placebo interventions. Images of those sections showing the highest numbers of immune (including B) cells were shows to 2 immunologists from the Gastroenterology division of the Erasmus Medical Centre (Rotterdam, the Netherlands). These experts were also of the opinion that none of the tissue sections did show any sign of infiltration of immune cells nor other visual signatures of an inflammatory response.

Preparation of Tissue Sections, LCM and Quantitative PCR. Frozen sections (7 μm thickness) were cut at −20 °C and 5 sections from one sample were transferred onto a glass slide (Superfrost plus, Fisher). The glass slide was transferred to a microslide box kept on dry ice and stored at −80 °C. Immediately before LCM, the glass slide with the frozen sections was taken from the freezer and thawed for 1 min at room temperature. The section was fixed in 70% ethanol for 10 sec at room temperature, followed by washing in nuclease-free water by dipping 10 times. The slide was stained with Histogen staining solution (Arcturus; MDS Analytical Technologies) for 10 sec and washed again in nuclease-free water. Then the slide was dehydrated in an ethanol/xylene gradient series: 10 dips 75% ethanol, 2 times 10 dips 95% ethanol, 1 min 95% ethanol, 3 times 1 min 100% ethanol, 3 times 1 min xylene. The sections were dried for 2 min at room temperature. A 7.5-μm laser beam was used (90 mW, 4.7 mSec) for laser capture microdissection using the Pix-Cell II with HS caps (Arcturus) for capture. Four hundred to 2,000 cells were shot for each sample. RNA was isolated from the LCM sample caps using the PicoPure RNA isolation kit (Arcturus) following manufacturer's recommendations. For a reverse transcription reaction, 200 ng of RNA (between 4 and 40 ng of RNA isolated from the cells isolated with LCM) was incubated at 65 °C for 5 min with 0.5 μg of random hexamers (Invitrogen) and 1 μL of 10 mM dNTP mixture. After 2 min on ice, the following was added: 5 μL of 5x first strand buffer, 2 μL of 0.1 M DTT, 200 Units SuperScript III reverse transcriptase, 40 units RNaseOUT RNase inhibitor (all Invitrogen) and water (final volume 20 μL). The reaction was incubated at 50 °C for 60 min and inactivated by heating at 70 °C for 15 min. cDNA samples were stored at −20 °C.

Quantitative PCR amplification was performed in 96-well plates on a 7500 Fast System (Applied Biosystems) using TaqMan primers and probes and 1 μL of 10-fold diluted RT product was used as a template. Assays were performed following the previously developed TaqMan assay reagents protocol (Applied Biosystems) with the following primers and probes: SLC11A2 (Hs00167207_m1), EGLN3 (Hs00222966_m1), CCL20 (Hs00171125_m1), CXCL2 (Hs00601975_m1), CD55 (Hs00167090_m1), SLPI (Hs00268206_m1), PFN4 (Hs00380763_m1), AQP10 (Hs01587666_g1) PSMB8 (Hs00544760_g1)and GAPDH (Hs02758991_g1). The following conditions were used: 50 °C for 2 min, 95 °C for 10 min, then 40 cycles at 95 °C for 15 sec, and 60 °C for 1 min. In each run, 4 standards were included with appropriate dilutions of the cDNA to make a standard curve and to quantify the samples. All measurements were done in duplicate. Significance of the difference in the gene expression levels was calculated by performing a paired 2-tailed *t* test on log-transformed data in Microsoft Excel.

SI Results

On the Interpretation of Differential Gene Expression. Both array (normalized data for each individual are available at National Center for Biotechnology Information's GEO, series number GSE11355) and QPCR (Fig. S1) did show that there was subject-to-subject variation in gene expression. For proper interpretation of mean differential gene expression across subjects, expression of relevant, interconnected (e.g., NFKB, IKB, SOCS3) genes was studied for each individual to correctly correlate differential expression of genes (e.g., encoding NF-κB subunits) to that of downstream targets (e.g., CXCL2). This way, we could be sufficiently sure that our interpretations were correct at the level of individual volunteers.

LCM-QPCR. Comparison of expression of genes in mucosal tissue biopsies and LCM-enriched epithelial cell pools showed that LCM contributed to the ability to measure cell-specific gene expression (Table S6).

Differentially Expressed Genes Measured by Microarray. Numbers and fold-change ranges of differentially expressed genes ($P <$ 0.05, based on Bayesian paired *t* test) after consumption of 3 bacterial preparation compared with placebo control or compared between each other were determined (Fig. S5).

Differentially Expressed Shared and Intervention-Specific Genes Visualized by Venn Diagrams. Venn diagrams showing the numbers of genes shared between different comparisons of bacterial preparations vs. placebo control (Fig. S6*a*), or between bacterial preparations (Fig. S6*b*).

Bibliosphere (Genomatix) analysis reveals differential major nodes regulating mucosal responses after consumption of 3 preparations of *L. plantarum*. (Fig. S7*a*). The dead- placebo comparison showed that nearly all interacting proteins were encoded by genes of which the expression was regulated by the activity of Jun, TNF-α and NF-κB. The stationary- placebo comparison showed that nearly all interacting proteins were encoded by genes of which the expression is driven by the activity of NF-κB (Fig. S7*b*). The midlog-placebo comparison showed that nearly all interacting proteins were encoded by genes of which the expression was driven by the activity of Cyclin D1, PARP1 and MYC. Note the absence of NF-κB (Fig. S7*c*).

1. Gentleman RC, *et al.* (2004) Bioconductor: Open software development for computational biology and bioinformatics. *Genome Biol* 5:R80.

2. Storey JD, Tibshirani R (2003) Statistical significance for genomewide studies. *Proc Natl Acad Sci USA* 100:9440–9445.

3. Dai M, *et al.* (2005) Evolving gene/transcript definitions significantly alter the interpretation of GeneChip data. *Nucleic Acids Res* 33:e175.
4. Irizarry RA, *et al.* (2003) Summaries of Affymetrix GeneChip probe level data. *Nucleic Acids Res* 31:e15.
5. Smyth GK (2004) Linear models and empirical Bayes methods for assessing differential expression in microarray experiments. *Stat Appl Genet Mol Biol* 3:Article3.
6. Gentleman RC, *et al.* (2004) Bioconductor: Open software development for computational biology and bioinformatics. *Genome Biol* 5:R80.
7. Higdon R, van Belle G, Kolker E (2008) A note on the false discovery rate and inconsistent comparisons between experiments. *Bioinformatics* 24:1225–1228.
8. Lee HK, Braynen W, Keshav K, Pavlidis P (2005) ErmineJ: Tool for functional analysis of gene expression data sets. *BMC Bioinformatics* 6:269.
9. Subramanian A, *et al.* (2005) Gene set enrichment analysis: A knowledge-based approach for interpreting genome-wide expression profiles. *Proc Natl Acad Sci USA* 102:15545–15550.
10. Mootha VK, *et al.* (2003) PGC-1alpha-responsive genes involved in oxidative phosphorylation are coordinately down-regulated in human diabetes. *Nat Genet* 34:267–273.
11. Patti ME, *et al.* (2003) Coordinated reduction of genes of oxidative metabolism in humans with insulin resistance and diabetes: Potential role of PGC1 and NRF1. *Proc Natl Acad Sci USA* 100:8466–8471.

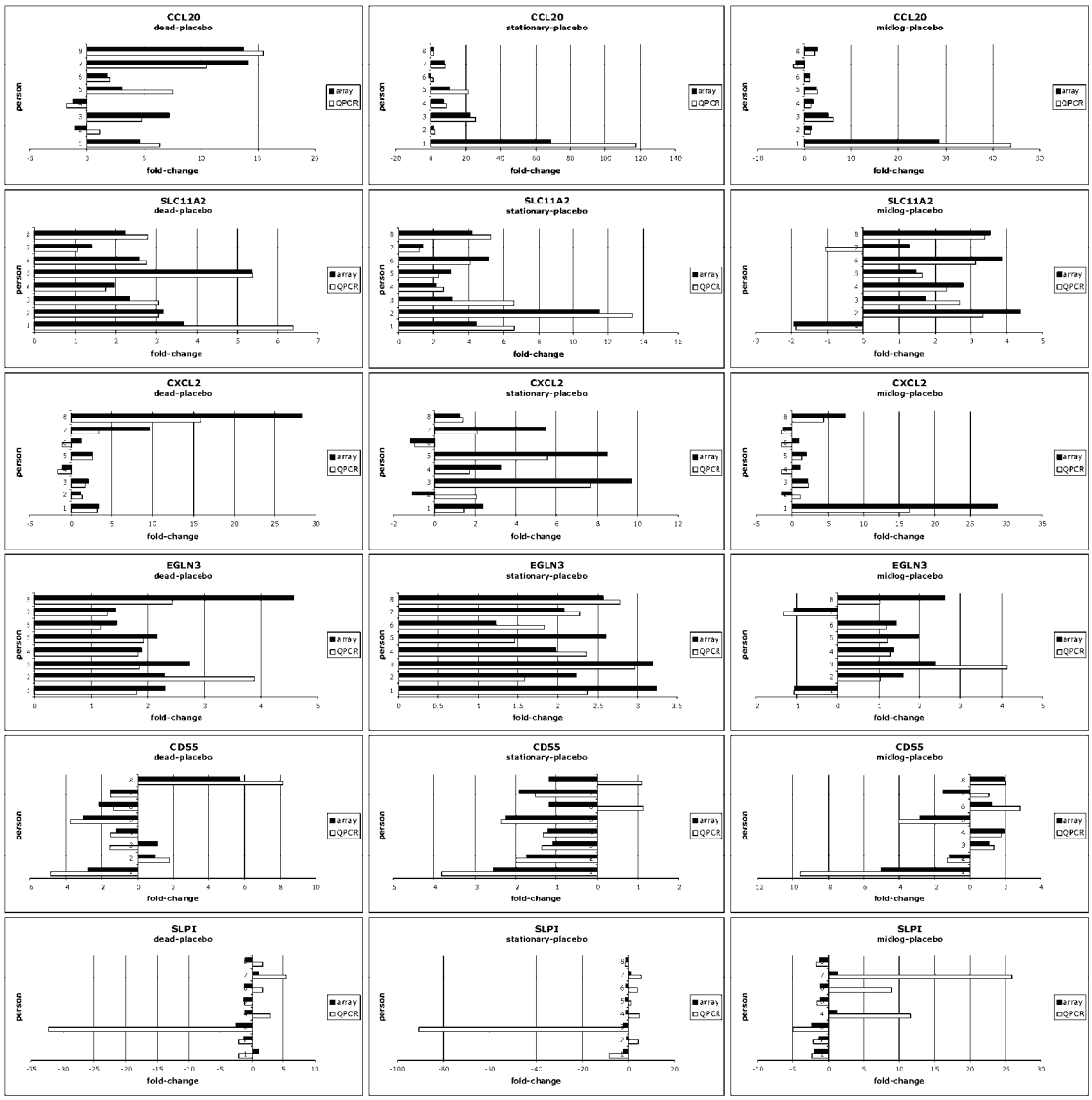

Fig. S1. QPCR results for six genes per individual volunteer.

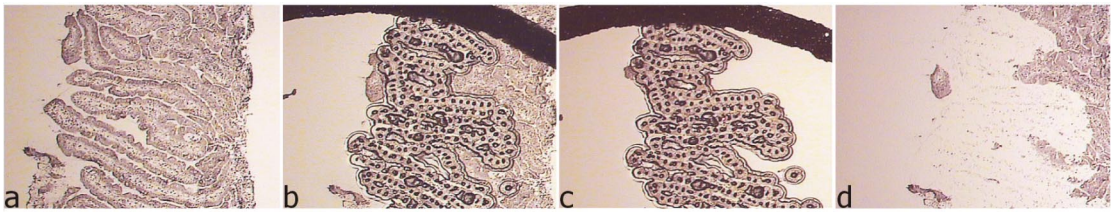

Fig. S2. Laser capture microdissection (LCM) treatment of human biopsies after consumption of *L. plantarum*. Images show an intact biopsy section (*a*), the same section after laser dissection (*b*), a dissected epithelial cell-enriched pool on the cover slide (*c*), and the remainder (cells from the lamina propria) of the section on the object slide (*d*). The dark curve in the upper part of images *b* and *c* is the upper part of the area that is covered by the laser. Magnification is 100×.

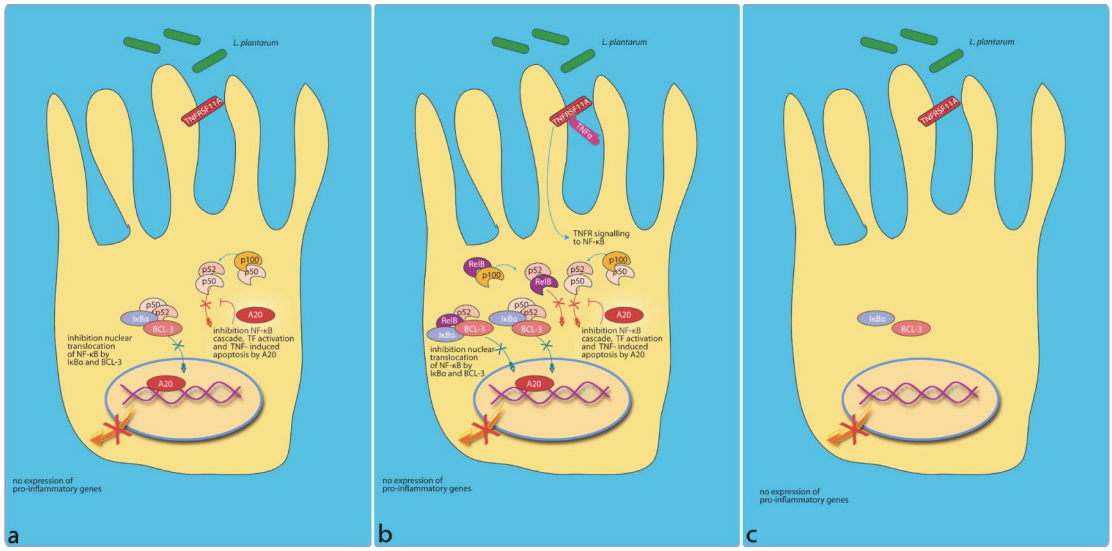

Fig. S3. Differential mucosal expression of NF-κB subunits after consumption of different growth stages of *L. plantarum*. Consumption of stationary bacteria (*a*) or dead bacteria (*b*) induces genes encoding NF-κB subunits and several inhibitors A20, IκB and BCL-3. In sharp contrast, only IκB and BCL-3 are expressed after consumption of midlog bacteria (*c*).

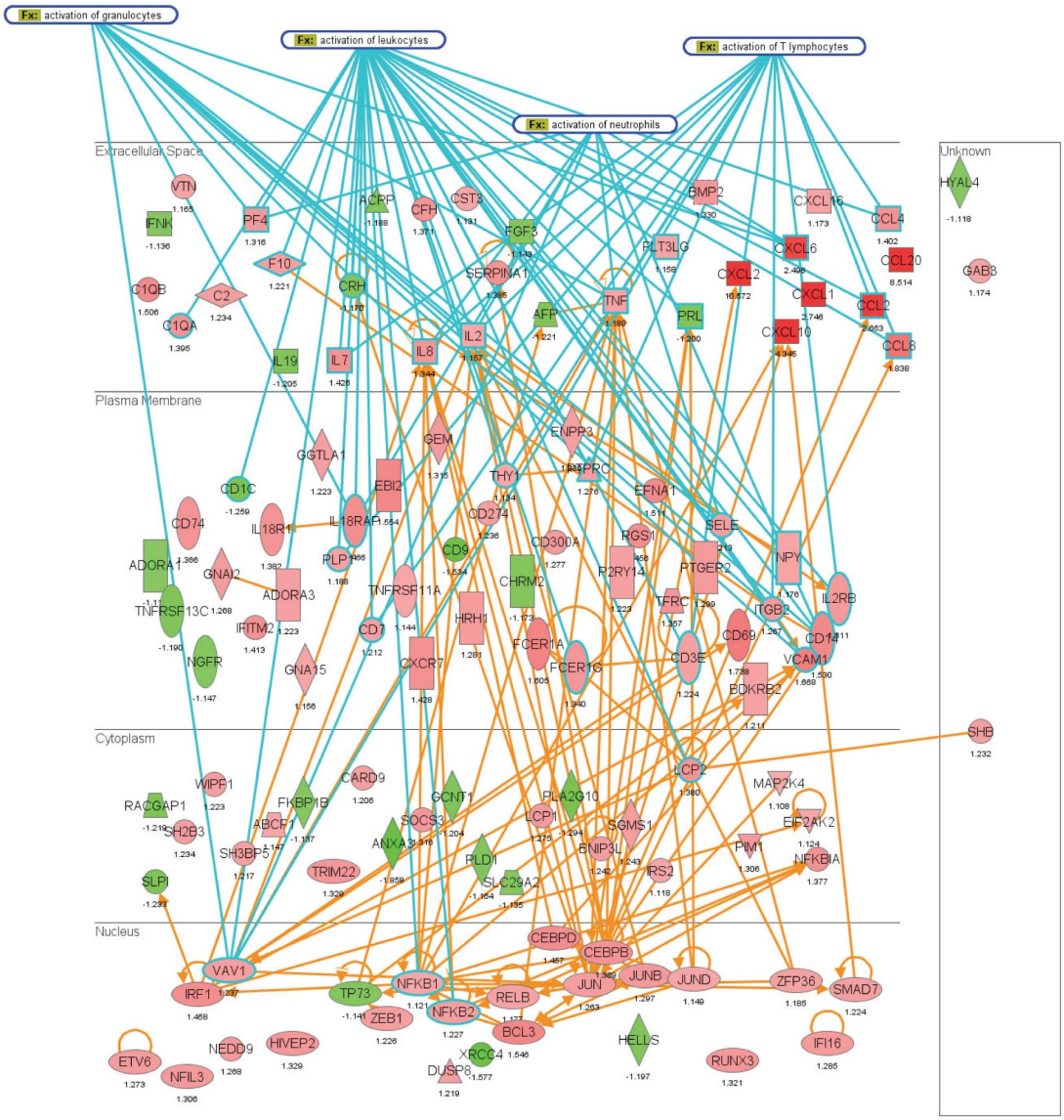

Fig. S4. IPA subcellular view of differential expression of genes participating in immune responses after consumption of 3 bacterial preparations. (*a*) The dead-placebo comparison included many genes involved in immune responses and immune and lymphatic tissue development; These are here represented in a protein–protein interaction map, together with cellular location. Less than a third of these were down-regulated. Many genes were involved in activation of immune cells. IPA subcellular view of differential expression of genes participating in immune responses after consumption of 3 bacterial preparations.

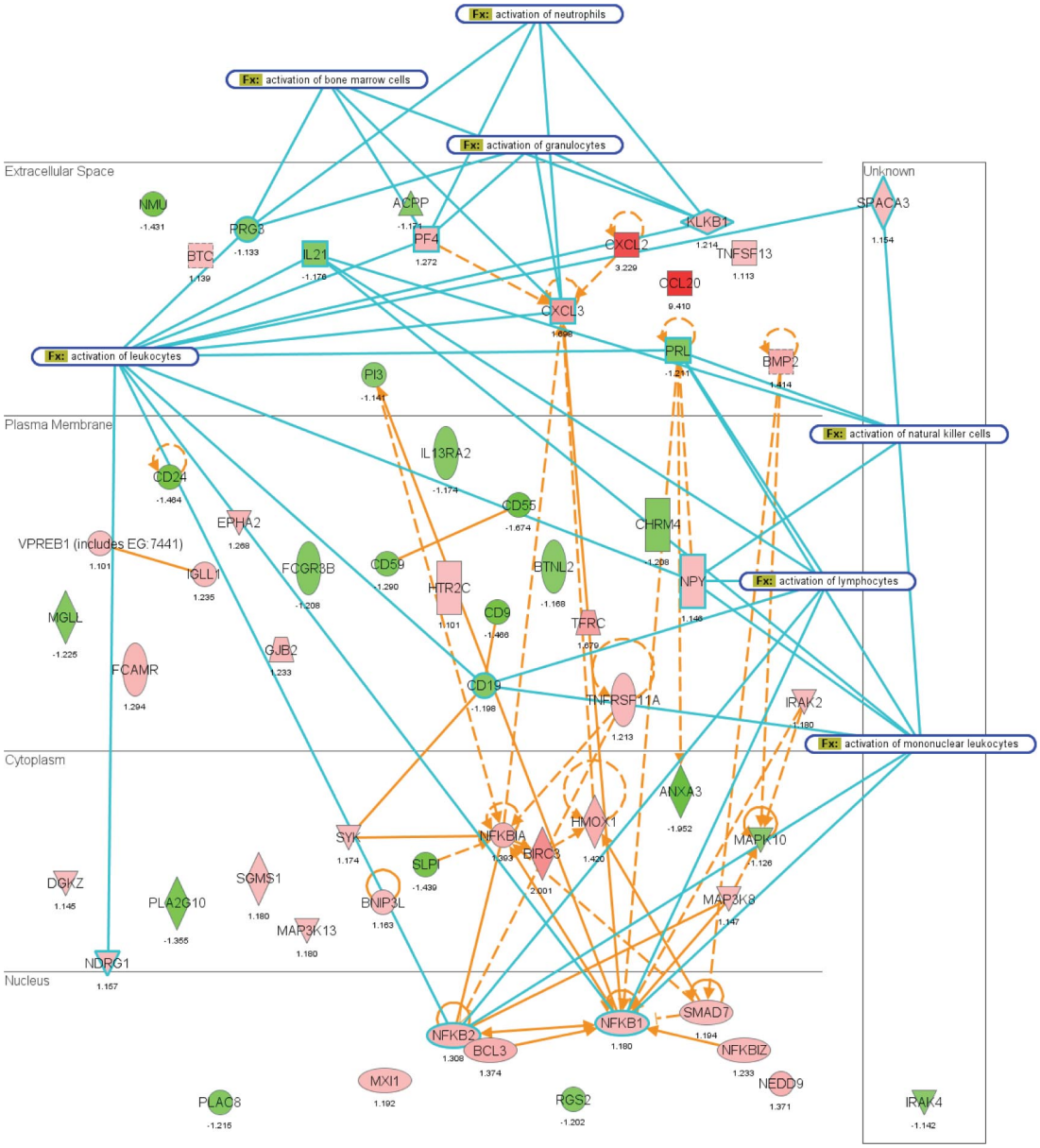

Fig. S4 (continued). (*b*) The stationary-placebo comparison included less genes involved in immune responses and immune and lymphatic tissue development compared with dead-placebo. Many of these were down-regulated. Compared with the dead-placebo comparison, less genes were involved in activation of immune cells. IPA subcellular view of differential expression of genes participating in immune responses after consumption of 3 bacterial preparations.

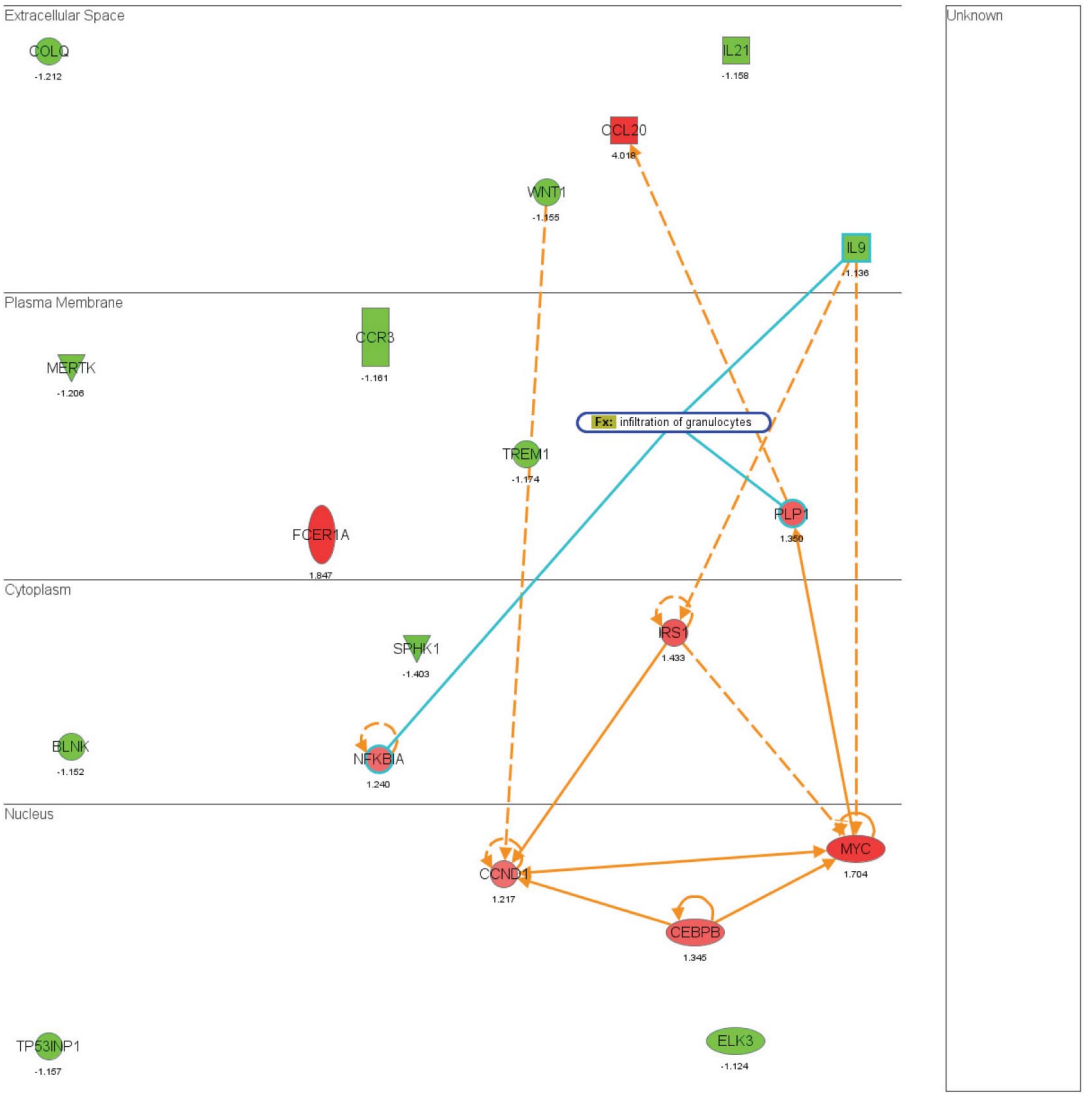

Fig. S4 (continued). (*c*) The midlog-placebo comparison included very few genes involved in immune responses and immune and lymphatic tissue development, most of these were down-regulated. Only few genes were involved in activation of immune cells.

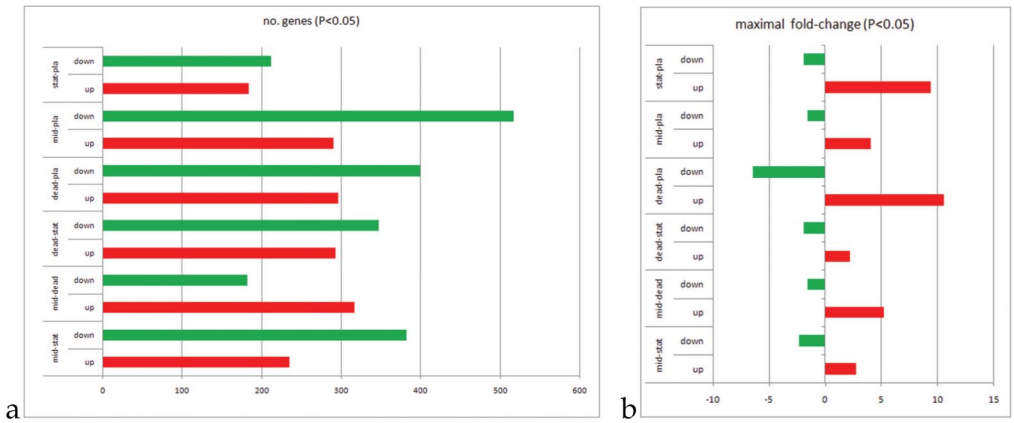

Fig. S5. Differentially expressed genes measured by micro-array. (*a*) Differentially expressed genes from the three comparisons of bacterial interventions versus placebo control treatments and the three bacterial interventions among one another. (*b*) Maximal fold-changes for each comparison.

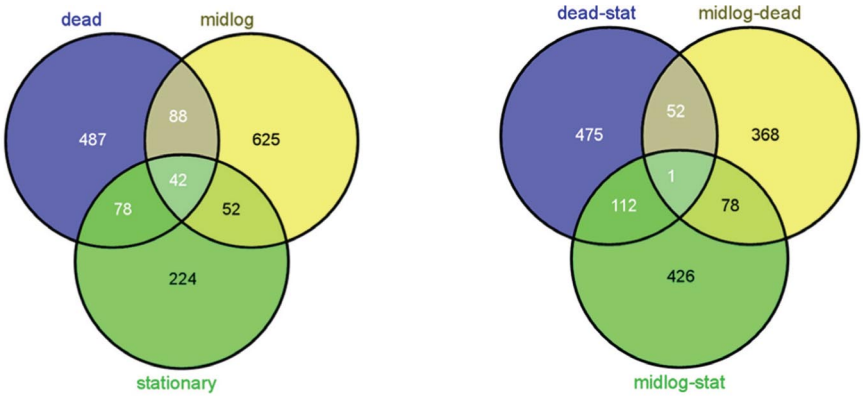

a b

Fig. S6. Venn diagrams showing the comparative response analysis of different bacterial interventions and placebo (*a*) or of different bacterial preparations (*b*).

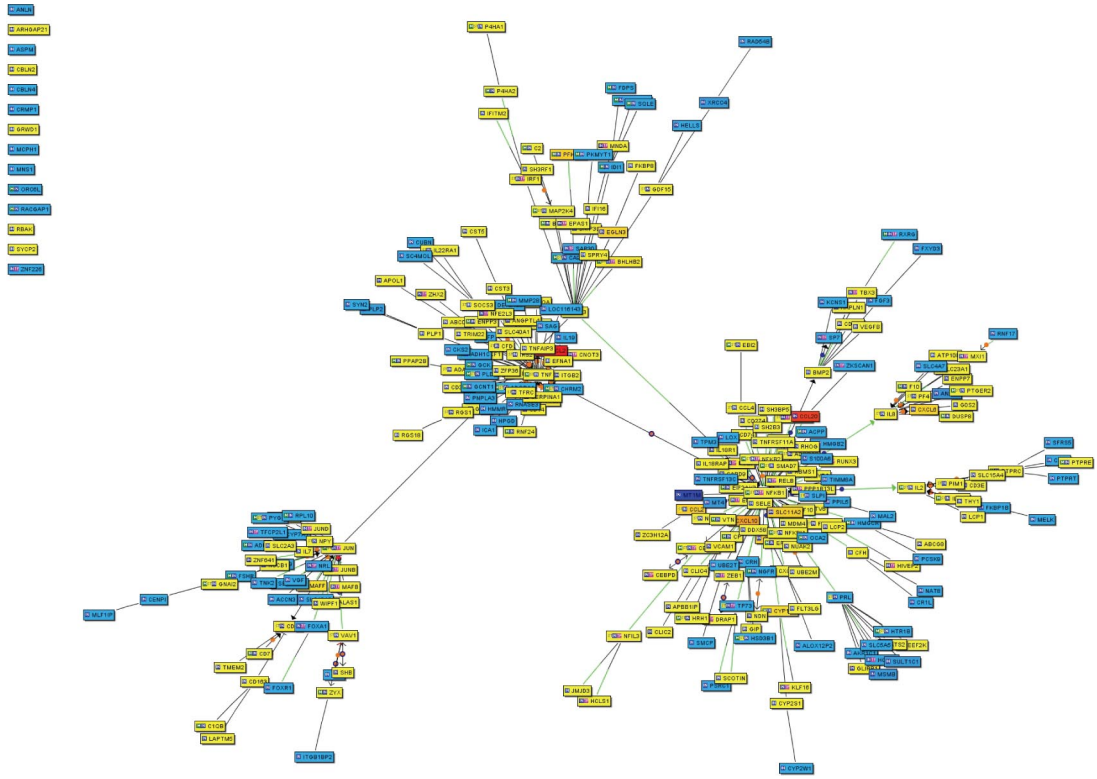

Fig. S7*a*. Bibliosphere analysis of mucosal responses after consumption of three preparations of *L. plantarum*. The comparison of dead-placebo (*a*), stationary-placebo (*b*), and midlog-placebo (*c*) are shown. Down-regulated genes are depicted in shades of blue, up-regulated genes are in shades of yellow to red.

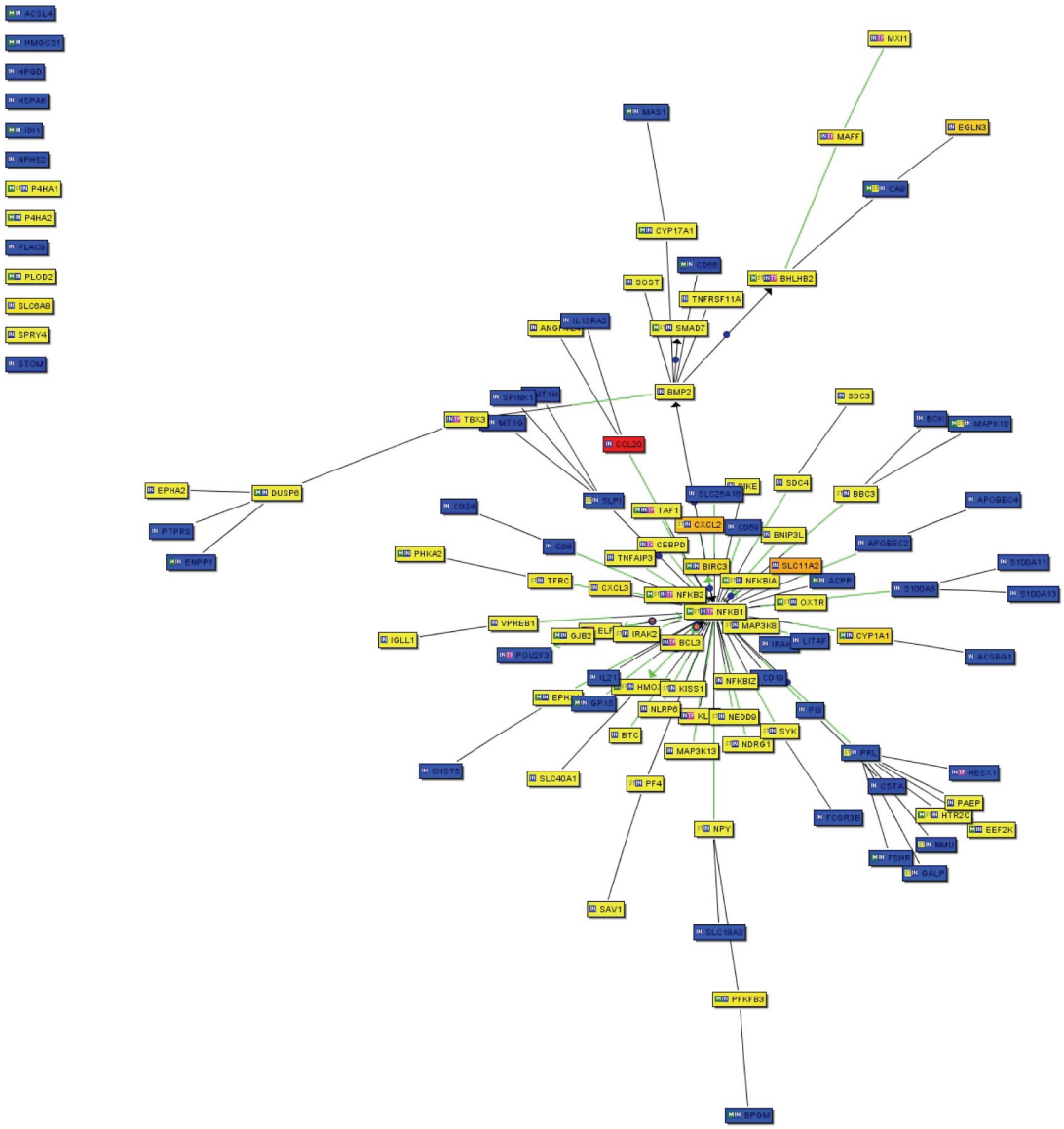

Fig. S7*b*. (continued)

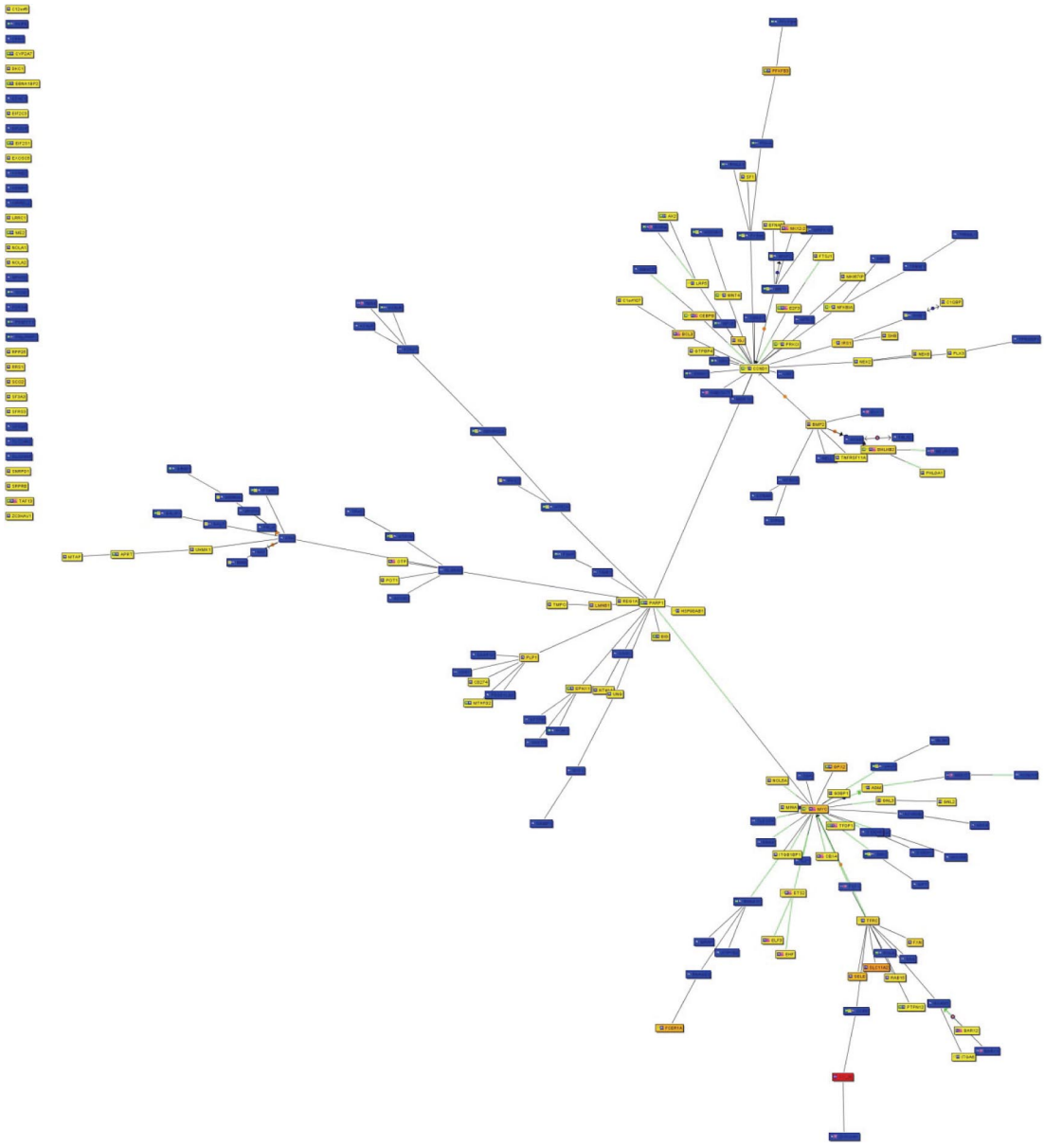

Fig. S7*c*. **(continued)**

Other Supporting Information Files

Table S1
Table S2
Table S3
Table S4
Table S5
Table S6